Title

Inversion of Sonic hedgehog action on its canonical pathway by electrical activity

Journal

Proceedings of the National Academy of Sciences of the United States of America, 112(13)

ISSN

0027-8424

Authors

Belgacem, Yesser H
Borodinsky, Laura N

Publication Date

2015-03-31

DOI

10.1073/pnas.1419690112

Peer reviewed

Inversion of Sonic hedgehog action on its canonical pathway by electrical activity

Yesser H. Belgacem[1] and Laura N. Borodinsky[1]

Department of Physiology and Membrane Biology and Institute for Pediatric Regenerative Medicine, Shriners Hospital for Children Northern California, University of California Davis School of Medicine, Sacramento, CA 95817

Edited by Charles F. Stevens, The Salk Institute for Biological Studies, La Jolla, CA, and approved February 20, 2015 (received for review October 13, 2014)

Sonic hedgehog (Shh) is a morphogenic protein that operates through the Gli transcription factor-dependent canonical pathway to orchestrate normal development of many tissues. Because aberrant levels of Gli activity lead to a wide spectrum of diseases ranging from neurodevelopmental defects to cancer, understanding the regulatory mechanisms of Shh canonical pathway is paramount. During early stages of spinal cord development, Shh specifies neural progenitors through the canonical signaling. Despite persistence of Shh as spinal cord development progresses, Gli activity is switched off by unknown mechanisms. In this study we find that Shh inverts its action on Gli during development. Strikingly, Shh decreases Gli signaling in the embryonic spinal cord by an electrical activity- and cAMP-dependent protein kinase-mediated pathway. The inhibition of Gli activity by Shh operates at multiple levels. Shh promotes cytosolic over nuclear localization of Gli2, induces Gli2 and Gli3 processing into repressor forms, and activates cAMP-responsive element binding protein that in turn represses *gli1* transcription. The regulatory mechanisms identified in this study likely operate with different spatiotemporal resolution and ensure effective down-regulation of the canonical Shh signaling as spinal cord development progresses. The developmentally regulated intercalation of electrical activity in the Shh pathway may represent a paradigm for switching from canonical to noncanonical roles of developmental cues during neuronal differentiation and maturation.

spinal cord development | Gli transcription factors | PKA | CREB | calcium-dependent activity

Sonic Hedgehog (Shh) signaling is a highly conserved pathway among vertebrates and invertebrates, known chiefly for its morphogenic role during embryonic development (1). Precise spatiotemporal regulation of signaling pathways is paramount for normal development and physiology of the nervous system. Indeed, abnormally low levels of Shh canonical signaling are responsible for diverse neurodevelopmental disorders like holoprosencephaly (2). On the other hand, constitutive activation of this pathway underlies the occurrence of several cancers including a subgroup of the pediatric brain tumor medulloblastoma (2), highlighting the importance of understanding the regulation of Shh canonical signaling.

This pathway results in the activation of the coreceptor Smoothened (Smo), a member of G-protein–coupled receptors leading to the recruitment of members of the zinc-finger transcription factor glioma-associated oncogenes Gli1 and Gli2 and inactivation of Gli3. As a consequence, expression of target genes such as *gli1* itself and Shh receptor *patched1* are enhanced (3).

During the early stages of spinal cord development, Shh is synthesized and secreted by the notochord and floor plate to form a ventrodorsal concentration gradient, imprinting a spatiotemporal profile of Gli activity (4, 5) that specifies neural progenitors (6–9). Despite persistence of Shh gradient and increased Shh levels as spinal cord development progresses (3, 10), Gli activity is switched off (3, 4) by unknown mechanisms. Some known inhibitory factors of Gli activity include Patched1, which operates in a negative feedback loop (11), and cAMP-dependent protein kinase (PKA), which acts by regulating Gli subcellular localization (12–15), processing, and degradation (16, 17).

Nervous system development is also accompanied by progressive acquisition of electrical activity that grows in complexity as neuronal differentiation advances (18–20). Even before synapses are formed, spontaneous Ca^{2+}-mediated electrical activity is present in developing neurons in many nervous system structures (21). This activity is important for numerous developmental processes such as proliferation, migration, axon guidance, and neurotransmitter specification (22–27). Interestingly, Shh elicits Ca^{2+} spikes in embryonic spinal neurons and thus regulates neuronal differentiation (28).

Whether the switch off of canonical Shh signaling and the emergence of spontaneous electrical activity are related events remains unclear. In this study, we demonstrate a previously unidentified mechanism by which electrical activity inverts Shh action on Gli through PKA recruitment as spinal cord development progresses.

Results

Shh-Ca^{2+} Spikes Signaling Axis Down-Regulates Gli Activity in the Developing Spinal Cord. To assess Gli transcriptional activity during spinal cord development, we expressed a Gli-luciferase reporter in *Xenopus laevis* embryos. Gli activity decreases during the transition from neural plate to embryonic spinal cord (Fig. 1*A*). Incubation with the Smo agonist, SAG, enhances Gli activity in the neural plate. Unexpectedly, in the spinal cord, SAG or Shh decreases Gli activity (71 ± 4% and 54 ± 12%, respectively, compared with control; Fig. 1*B*), demonstrating a switch in Shh recruitment of Gli transcription factors as spinal cord development progresses.

Significance

Morphogenic proteins drive the formation and patterning of tissues during embryonic development. Once tissues are formed, their cells progressively differentiate to perform the required specialized functions of the maturing tissue. Whether this transition is accompanied by changes in morphogen signaling remains unclear. Here we identify a striking inversion in Sonic hedgehog (Shh) action on its canonical Gli-dependent pathway driven by the emerging electrical activity in differentiating spinal neurons. This mechanism may allow for switching off Shh proliferative action and thus may prevent pediatric brain tumor formation and occurrence of neurodevelopmental defects.

Author contributions: Y.H.B. and L.N.B. designed research; Y.H.B. performed research; Y.H.B. analyzed data; and Y.H.B. and L.N.B. wrote the paper.

The authors declare no conflict of interest.

This article is a PNAS Direct Submission.

Freely available online through the PNAS open access option.

[1]To whom correspondence may be addressed. Email: lnborodinsky@ucdavis.edu or yhbelgacem@ucdavis.edu.

This article contains supporting information online at www.pnas.org/lookup/suppl/doi:10.1073/pnas.1419690112/-/DCSupplemental.

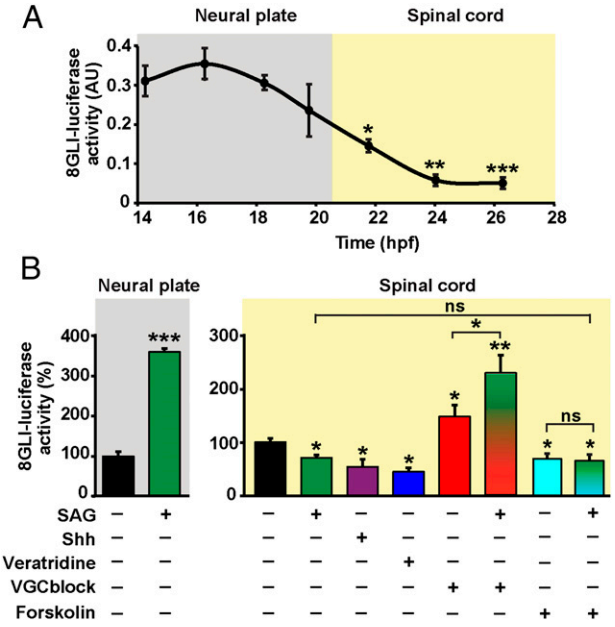

Fig. 1. The Shh-Ca^{2+} spike signaling axis down-regulates Gli activity in the developing spinal cord. (*A*) Neural plates and spinal cords from embryos expressing a Gli activity reporter (8GLI-luciferase) were dissected at different developmental stages and processed for luciferase signal measurements. Graph shows mean ± SEM firefly luciferase normalized to Renilla luciferase activity levels in neural tissue at indicated developmental stages; $n \geq 5$, $^{*}P < 0.05$, $^{**}P < 0.005$, and $^{***}P < 0.001$ compared with early neural plate stage [14.25 hours postfertilization (hpf)]. (*B*) Neural plates and spinal cords from embryos expressing 8GLI-luciferase were incubated for 8 h with the indicated agents and processed for luciferase activity measurements. Graphs show mean ± SEM percentage of normalized luciferase intensity compared with control (incubated with vehicle only) in each developmental stage; $n \geq 5$, $^{*}P < 0.05$, $^{**}P < 0.005$, and $^{***}P <$ 5E-9; ns: not significant.

Down-regulation of Gli activity in the developing spinal cord coincides with the appearance of spontaneous Ca^{2+}-mediated electrical activity (22) that is modulated by Shh (28). Therefore, we determined whether electrical activity has an inhibitory effect on Gli activity. Increasing Ca^{2+} spike activity by veratridine (22, 28), a voltage-gated Na^{+} channel agonist, diminishes Gli–luciferase levels in the spinal cord (45 ± 6% compared with control). In contrast, blocking electrical activity using voltage-gated Na^{+} and Ca^{2+} channel blockers (VGCblock) (22, 28) enhances Gli transcriptional activity (Fig. 1*B*). In addition, blockade of Ca^{2+} spike activity in the spinal cord increases transcript levels of Patched 1 (Fig. S1), a direct target gene of the canonical Shh pathway. These results show that Ca^{2+} spikes inhibit Gli activity. Moreover, the blockade of Ca^{2+} spikes reverses the SAG-induced decrease in Gli transcriptional activity in spinal cord samples (Fig. 1*B*), indicating that suppression of electrical activity in the spinal cord restores Smo-induced canonical recruitment of Gli, characteristic of earlier developmental stages. In the neural plate, stimulating voltage-gated Na^{+} channels with veratridine does not increase the level of Ca^{2+} activity (Fig. S2*A*) and, accordingly, does not affect Gli activity (Fig. S2*B*).

These results demonstrate that Ca^{2+} spikes inhibit Gli activity and prevent Shh-triggered canonical pathway.

Shh Switches Its Action on PKA Activity During Spinal Cord Development. Ca^{2+}-dependent electrical activity is the trigger of many intracellular signaling cascades in neurons; among them, PKA is an important transducer of electrical activity (29). Additionally, PKA is a major inhibitor of the canonical Shh pathway in vertebrates (30–33), and expressing a dominant-negative PKA mimics an ectopic Shh-induced ventralized spinal cord phenotype in mice (32). We find that stimulating PKA with the adenylate cyclase activator forskolin inhibits Gli activity (Fig. 1*B* and Fig. S2*B*). Moreover, PKA activation also decreases transcription of *patched 1*, even in neural plate samples where Gli activity is at its peak (Fig. S1). Reciprocally, Shh inhibits PKA in early stages of mouse spinal cord development (34). We find that, although SAG inhibits PKA activity in the neural plate (82 ± 7% compared with control), it enhances PKA activity in the spinal cord (Fig. 2*A*). Using the FRET-based PKA activity reporter in dissociated cells derived from neural plate or spinal cord (Figs. S3 and S4), we find that, like SAG, Shh enhances PKA activity in spinal cord cells within minutes of stimulation (Fig. 2*B*). In contrast, it decreases the signal of FRET-based PKA reporter in neural plate cells, where most of the cells are undifferentiated neural progenitors (Fig. 2*B* and Fig. S4). Enhancing Ca^{2+} spikes increases PKA activity in the spinal cord, and simultaneously enhancing Smo and Ca^{2+} spikes does not increase PKA activity any further than singly stimulating these pathways (Fig. 2*A*). Accordingly, occlusion experiments show that activating Smo and PKA simultaneously does not lead to an additional decrease in Gli activity compared with the effect of stimulating Smo or PKA alone (Fig. 1*B*). In the neural plate, stimulating voltage-gated Na^{+} channels does not affect PKA activity in contrast to the increase observed when stimulating PKA with forskolin (Fig. S5).

These results suggest that activation of the Shh pathway in the embryonic spinal cord enhances PKA activity through a Smo and Ca^{2+} spike-dependent mechanism and that this mechanism contributes to switching off Gli activity.

Shh Facilitates Processing of Gli2/3 in the Embryonic Spinal Cord and Inhibits Gli2 Nuclear Localization in Spinal Cord Cells. To determine the mechanisms by which Shh inhibits Gli activity in the spinal cord, we investigated different aspects of Gli activity regulation that are known to be mediated by PKA, including post-translational processing and subcellular localization (12–17). We evaluated the processing of Gli2/3 in the embryonic spinal cord by assessing the relative levels of full-length and cleaved (repressor) forms of endogenous Gli3 and exogenously expressed mGli2-GFP (35). We find that Smo activation leads to an increase in the ratio of repressor to full-length Gli3 and Gli2 protein levels (254 ± 76% and 332 ± 64% increase, respectively; Fig. 3*A* and Fig. S6), suggesting that Shh signaling may inhibit Gli activity by favoring the processing of Gli2 and Gli3.

Assessment of Gli localization shows that Gli2 is present mainly in nuclei in the neural plate whereas Gli2 immunolabeling is also present in the cytosol of spinal cells (Fig. 3*B*). To determine the dynamics of Gli2 subcellular localization, we confocally imaged dissociated embryonic spinal neurons from mGli2-GFP–expressing embryos (Fig. S7 *A* and *B*). Results reveal that SAG leads to a decrease in Gli2 nuclear localization in spinal neurons concomitant with an increase in cytosolic Gli2 levels within 7 min of SAG addition (Fig. 3 *C* and *E*). This SAG-induced effect on Gli2 localization is mimicked by Shh or by activating PKA (Fig. 3*E* and Fig. S7*C*) and prevented by inhibiting PKA (Fig. 3 *D* and *E* and Fig. S7*C*). These results demonstrate that Smo activation promotes, through PKA, the localization of Gli2 to the cytosol in spinal cord cells, thus preventing Gli2 transcriptional activity.

Shh Activates CREB, Which Represses *gli1* Transcription in the Developing Spinal Cord. To examine a potential change in the transcriptional regulation of Gli1 expression during spinal cord development, we identified typical electrical activity-responsive elements within the regulatory region of the h*gli1* gene (reg-h*gli1*) that are conserved across species. Three of the conserved sites are consensus and variant cAMP-responsive elements (CREs), which are potential targets of CREB (36, 37), a transcription factor recruited by electrical Ca^{2+}-mediated activity and phosphorylated by PKA

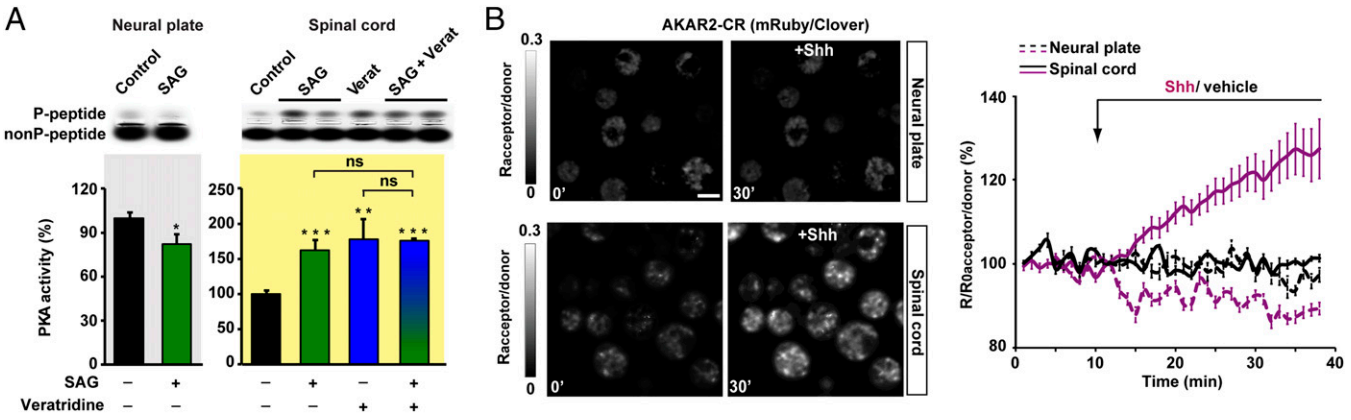

Fig. 2. Shh inverts its action on PKA activity during spinal cord development. (*A*) Neural plates and spinal cords were incubated for 30 min with indicated agents and processed for PKA activity measurements with a nonradioactive PKA assay. Images are representative examples of the PKA activity assay. Graph shows mean ± SEM PKA activity (P-substrate/non–P-substrate optical density ratio) for the indicated treatments; $n \geq 5$, $^{*}P < 0.05$, $^{**}P < 0.001$, $^{***}P <$ 5E-5 compared with control (incubated with vehicle only); ns: not significant; verat: veratridine. (*B*) Dissociated neural plate and spinal cord cells from AKAR2-CR–expressing 14.25- and 21-hpf embryos were time-lapse imaged every 30 s. (*Left*) Representative ratiometric (acceptor-mRuby/donor-Clover) images of cells before and 30 min after addition of 10 nM Shh. Grayscale bar represents acceptor/donor ratio increasing from black to white. Traces represent mean ± SEM percentage change in emission ratio; $n \geq 29$ cells per condition. (Scale bar: 20 μm.)

(38). Interestingly, CREB appears more activated (P-CREB) in the spinal cord than in the neural plate (Fig. S8*A*). We find that enhancement of Shh signaling increases P-CREB levels in the spinal cord (Fig. 4*A*), mimicking the effect of activating PKA (Fig. S8*B*). We then assessed the effect of electrical activity-responsive elements on *gli1* transcription by designing a luciferase gene reporter downstream of wild-type reg-h*gli1* or a mutated version in all three conserved sites (Fig. 4*B*). We find that the wt-reg-h*gli1*-luciferase reporter signal is higher in the neural plate compared with the spinal cord (Fig. 4*C* and Fig. S9), in agreement with our findings using the 8GLI-luciferase reporter (Fig. 1*A*) and those of others (3, 4). Enhancing Shh signaling by treating samples with SAG increases *gli1* transcription in neural plate samples whereas it decreases it in the spinal cord (Fig. 4*C*). To assess the effect of CREB on *gli1* transcription, we overexpressed CREB, which imposes high levels of P-CREB in developing embryos (Fig. S8*C*) and determined the levels of reg-h*gli1*-luciferase reporter in neural plate and spinal cord samples. Results show that P-CREB inhibits *gli1* transcription in neural plate and spinal cord. Moreover, enhancing P-CREB at neural plate stages decreases wt-reg-h*gli1*-luciferase signal to spinal-cord-stage levels. P-CREB overexpression occludes both the increase and the decrease in *gli1* transcription induced by SAG in neural plate and spinal cord, respectively (Fig. 4*C*). Mutating putative CREB-binding sites prevents the overexpressed P-CREB–induced decrease in reg-h*gli1*-luciferase signal, and enhances the basal reporter signal in the spinal cord (Fig. 4*C*), demonstrating that these are binding sites for repressors of *gli1* transcription. In contrast, signal levels of wild-type and mutant reporters are comparable in neural plate stages (Fig. 4*C*), suggesting that this negative regulation of *gli1* transcription is not active at these developmental stages. Additionally, enhancing PKA activity decreases the wt-reg-h*gli1* signal in spinal cord but has no significant effect on the signal of the mutant reporter (Fig. 4*C*), indicating that these regulatory elements in the *gli1* gene contribute to the inhibitory modulation of *gli1* transcription through PKA.

Gli activity is also sensitive to CREB levels, as revealed by comparing 8GLI-luciferase reporter signal in CREB-overexpressing and wild-type neural plates (Fig. S10).

These results suggest that Shh signaling represses *gli1* transcription in the embryonic spinal cord by activating CREB through PKA and that the regulatory regions of *gli1* integrate Gli and electrical activity signals.

Discussion

The transition from neural plate to spinal cord is accompanied by the appearance of electrical activity (22) concurrently with down-regulation of the Shh canonical pathway (3, 4). Here we find that the intercalation of Ca^{2+} spikes in Shh signaling inverts its action on Gli transcription factors (Fig. 5). Shh enhances electrical activity in the developing spinal cord (28), leading to Ca^{2+} influx and activation of several protein kinases, including PKA, which leads to phosphorylation and activation of CREB as shown in this study and others (39). In the adult brain where neural cells at different stages of maturation coexist, electrical activity and P-CREB are progressively up-regulated as newborn neurons differentiate (40). Similarly, we find that mutating potential binding sites for CREB in neural plate samples does not affect *gli1* transcription, whereas in the spinal cord these mutations reveal a repressive character for these regulatory sites. This suggests that CREB activity is progressively recruited during neuronal differentiation in the embryonic spinal cord. Although CREB is mostly known as an activator, it has been found to inhibit transcription, and whether it acts as a repressor depends on its phosphorylation status (41), the partners recruited in transcriptional complexes (42), and the regulatory region of the gene to which CREB binds (43). Alternatively, CREB negative effect on *gli1* transcription may be indirect by inducing expression of a repressor (44).

The switch off of the canonical Shh pathway is also implemented at the level of regulating Gli subcellular localization and posttranslational processing, all converging in inhibiting Gli activity (Fig. 5). The mechanisms underlying this multilayered inhibition triggered by Shh involve PKA activation, which is recognized as an inhibitor of the Shh canonical pathway (30–33). On the other hand, Smo activation recruits heterotrimeric $G\alpha_i\beta\gamma$ proteins (28, 45), which inhibits adenylate cyclase, eventually leading to decreased PKA activity. These findings may be explained by considering that different types of adenylate cyclase and PKA are tightly compartmentalized in the cell. In particular, Smo activation inhibits pools of PKA located at the base of the primary cilium in the developing mouse neural tube and cerebellar granule neural precursors (12, 46). In contrast, in the developing spinal cord, Smo activation leads to an increase in cytosolic Ca^{2+} spikes (28) that enhance total levels of PKA activity, as shown here.

The regulatory mechanisms for inhibiting Gli activity identified in this study likely operate with different spatiotemporal

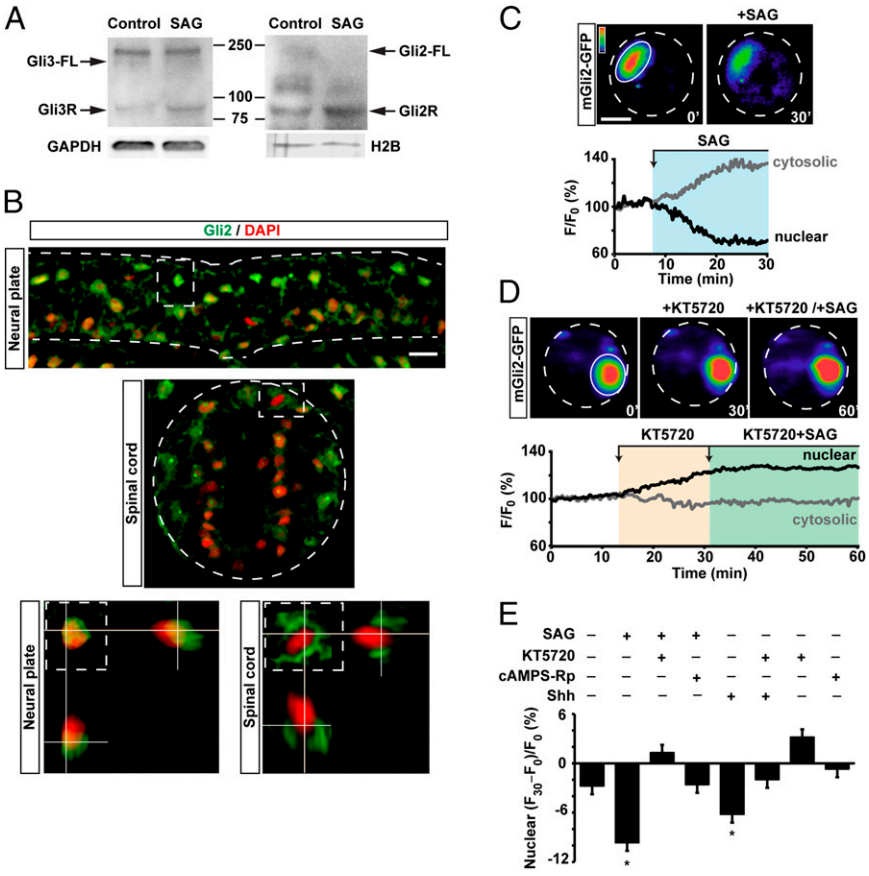

Fig. 3. Shh facilitates processing of Gli2/3 and inhibits Gli2 nuclear localization in spinal neurons. (*A*) Representative examples of Western blot assays from whole-cell spinal cord homogenates from wild-type and mGli2-GFP–expressing embryos probed with anti-Gli3 and anti-Gli2, respectively. H2B or GAPDH were used as loading controls. Samples were incubated in the absence or presence of 100 nM SAG for 4 h. Gli-FL: Gli full length; GliR: Gli repressor. (*B*) Shown are representative examples of transverse sections of neural plate and spinal cord (outlined) from wild-type embryos immunostained for Gli2. Dashed squares are areas magnified in adjacent panels. Orthogonal views are shown to demonstrate subcellular localization of Gli2 immunolabeling. (*C*–*E*) Dissociated spinal cord cells from mGli2-GFP–expressing 21-hpf embryos were time-lapse imaged every 15 s. (*C* and *D*) Representative examples of imaged cells under indicated treatments. Contour of imaged cells and nuclei are indicated with dashed and solid lines, respectively. Color scale bar represents fluorescence intensity increasing from purple to red. Traces represent changes in nuclear (black) and cytosolic (gray) fluorescence for the given examples. (*E*) Graph shows mean ± SEM percentage of final change in nuclear mGli2-GFP fluorescence intensity upon addition of indicated agents; $n \geq 27$ cells per condition; $^*P < 0.05$ compared with control (vehicle only). (Scale bars: 20 μm in *B* and 10 μm in *C*.)

resolution and ensure effective down-regulation of the canonical Shh signaling as spinal cord development progresses. It is known that the Shh receptor Patched acts as a negative feedback regulator of canonical signaling, assuring precise patterning of spinal neural progenitors (4, 5). However, such a regulatory mechanism predicts temporal adaptation of cells to Shh (4, 5) rather than switching off of canonical signaling. The long-term down-regulation of canonical Shh signaling may have important implications. Inhibition of Gli activity may be necessary for engaging Shh in distinct signaling pathways and functions of the maturing and adult tissues. Noncanonical Shh signaling (47, 48) is implicated in regulation of muscle and brown-fat metabolism (49) and, in the spinal cord, participates in neurotransmitter specification and axon guidance (28, 50). Interestingly, in the adult ventrolateral nucleus of the *tractus solitarius*, Shh acutely modulates neuronal excitability (51). Our findings on Shh-induced activation of CREB, a master transcription factor for neural activity-dependent regulation of gene expression (39), predict that Shh will participate in neural functions of the maturing and adult nervous system.

Materials and Methods

Animals. Wild-type and experimental *X. laevis* embryos were used at stages 12.5–34 [14.25–45 h postfertilization (hpf)]. Neural plate stages correspond to 14.25–20.75 hpf embryos, as indicated in Fig. 1. For most experiments, neural plates and spinal cords were dissected from 16.25 hpf (stage 14) and 26.25 hpf (stage 24) embryos, respectively, unless indicated otherwise. Procedures involving animal handling and use were approved by the University of California, Davis, Institutional Animal Care and Use Committee.

DNA Constructs. Gli2-GFP was obtained from P. Beachy, Stanford School of Medicine, Stanford, CA (Addgene plasmid 37672). CREB was obtained from M. Montminy, The Salk Institute for Biological Studies, La Jolla, CA (Addgene plasmid 22968), which after subcloning was in vitro transcribed for mRNA injections. AKAR2-CR was obtained from M. Lin, Stanford School of Medicine, Stanford, CA (Addgene plasmid 40255). PKA catalytic subunit α was obtained from S. Taylor, University of California, San Diego, La Jolla, CA (Addgene plasmid 14921). The wt-reg-h*gli1*-luc plasmid was obtained by inserting the DNA fragment corresponding to the 2,861 bp upstream of the ATG of the human *gli1* first untranslated exon into pGL4.23[luc2/minP] (Promega, E8411) using KpnI and EcoRV. The mut-reg-h*gli1*-luc plasmid was obtained by mutating the three CREs in the reg-h*gli1*-luc plasmid as described in Fig. 4*B*.

Luciferase Assay. Gli activity or regulation of *gli1* transcription was measured using a firefly luciferase-based Gli-reporter assay (8GLI-luciferase, Cignal reporter Gli, Qiagen) or a regulatory region of *gli1*-firefly luciferase reporter (reg-h*gli1*-luc), respectively. Firefly luciferase constructs along with the normalizing CMV enhancer-controlled renilla luciferase construct (Cignal Gli reporter, Qiagen or pRL-CMV Vector, Promega) were injected in two-cell-stage embryos. Neural plates or spinal cords from 14.25- to 45-hpf embryos were dissected and processed for luciferase assay reading or incubated with drugs for 8 h. Concentrations of drugs used were the following: 100 nM SAG (Smo agonist, Calbiochem); VGCblock: 20 nM calcicludine (Calbiochem), 1 μM ω-conotoxin–GVIA, 1 μM flunarizine, and 1 μg/mL tetrodotoxin (Sigma); 1 μM veratridine (voltage-gated Na^+ channel agonist, Sigma); 10 μM forskolin (adenylyl cyclase agonist, Tocris); and 10 nM human Shh recombinant peptide (N terminus, C24II, catalog no. 1845-SH, R&D Systems). Samples were homogenized in 20 μL of passive lysis buffer (Dual-Luciferase Reporter Assay System, Promega). Firefly and renilla luciferase activities were quantified using a Microbeta Trilux luminescence counter (Perkin-Elmer) after addition of the LARII and Stop&Glow reagents, respectively (Dual-Luciferase Reporter Assay System, Promega). Firefly/renilla activity ratio was then calculated for each sample.

Quantitative RT-PCR. Total RNA was isolated from dissected neural plates (14.75-h-old embryos) or spinal cords (26-h-old embryos) previously incubated for 8 h with 20 μM forskolin (neural plates), voltage-gated Na^+ and Ca^{2+} channel blockers (VGCblock listed above, spinal cords), or vehicle only (control, neural plates, and spinal cords) using the RNeasy kit (Qiagen). cDNA was synthesized from 5 μg of mRNA using the QuantiTect Reverse Transcription Kit (Qiagen) according to the manufacturer's instructions. Relative

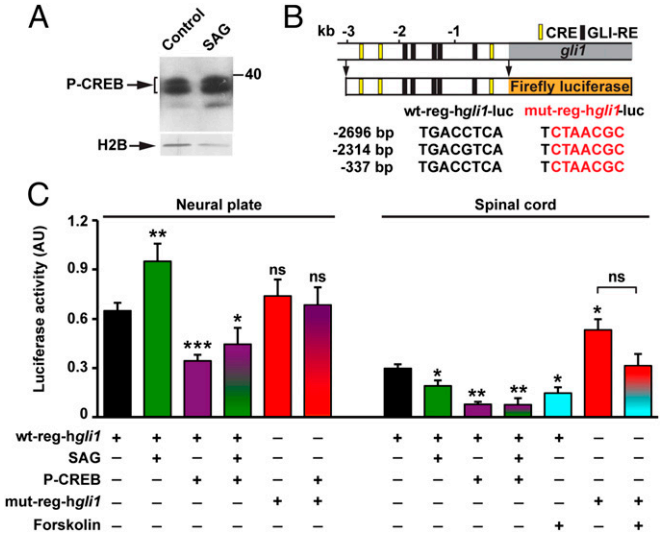

Fig. 4. Shh activates CREB that represses *gli1* transcription in the developing spinal cord. (*A*) Shown is a representative Western blot assay from spinal cord samples incubated in the absence or presence of 100 nM SAG for 40 min and immunoprobed for activated CREB (Ser133-P-CREB) and H2B as loading control. (*B*) Schematic of luciferase reporters used to assess regulation of *gli1* transcription. Sequences of three identified CREs and their relative positions to the ATG of the human *gli1* first untranslated exon. (*C*) Neural plates and spinal cords from embryos expressing wt-reg-h*gli1*-luciferase or mut-reg-h*gli1*-luciferase in the absence or presence of CREB overexpression were incubated with indicated agents or vehicle for 8 h and processed for luciferase activity measurements. Graph shows mean ± SEM normalized luciferase intensity; $n \geq 5$; $^{*}P < 0.05$, $^{**}P < 0.005$, and $^{***}P < 0.00005$; ns: not significant.

Patched 1 and ornithine decarboxilase (ODC) transcript levels were then assessed using 5 μg of cDNA per sample for quantitative PCR (Stratagene Mx3005P). QuantiTect SYBR Green PCR Kit (Qiagen) was used for neural plates according to the manufacturer's instructions, and a semiquantitative PCR was used for spinal cord samples due to below-threshold transcript levels for the SYBR Green-based assay. Primers specific for Patched 1 were forward (5′-CTAAAGCGCACAGGAGCAAGC-3′) and reverse (5′-CAGGCTGTAGCGTGTATTGTC-3′). Primers for ODC were forward (5′-GCCATTGTGAAGACTCTCTCCATT-3′) and reverse (5′-ATCCGCTCGGGGGAAACTCC-3′).

Calcium Imaging in Neural Plate Stages. Messenger RNA of the genetically encoded Ca^{2+} sensor GCaMP6s was injected into two-cell stage embryos (3 ng mRNA/embryo). Embryos were allowed to grow until neural plate stages (14.25 hpf) and then imaged under a confocal microscope with an acquisition rate of 0.2 Hz for 30 min in the absence and presence of 1 μM veratridine, voltage-gated Na^{+} channel agonist. The number of Ca^{2+} transients before and after treatment was compared, and significance was assessed by paired *t* test.

PKA Activity Assay. PKA activity was measured using a PepTag Non-Radioactive Protein Kinase Assay specific for PKA (Promega). After dissection, four neural plates or four spinal cords from 14.25- or 26-hpf embryos were incubated for 30 min with drugs or vehicle only (control). Concentrations of drugs used were as for the luciferase assay. Following the manufacturer's instructions, samples were homogenized in 20 μL of cold PKA extraction buffer, and total protein was measured using a BCA kit (Thermo Scientific) for normalization. Equal amounts of total protein in treated and control samples were incubated for 45 min with the Peptag reaction mix without PKA activator (5 μL buffer, 2 μL Peptag peptide, 1 μL peptide protector, and a variable volume of sample for a total volume of 25 μL per reaction). Negative and positive controls were performed according to manufacturer instructions. Samples were then run on electrophoretic gel for 25 min.

FRET Assay. AKAR2-CR and mouse PKA catalytic subunit-α mRNAs were injected into one-cell-stage embryos. The overexpressed PKA catalytic subunit is regulated by the regulatory PKA subunit (52) and is used here to amplify the signal of the PKA activity FRET reporter (AKAR2-CR). Neural plates or spinal cords from 14.25- or 26-hpf AKAR2-CR-expressing embryos were then dissected, dissociated, and plated in vitro as previously described (26, 28) for 2 h. Cells were imaged every 30 s under a confocal microscope (Nikon A1) using a 488-nm excitation laser. Fluorescence emitted from Clover (donor) and mRuby (acceptor) were quantified using spectral detection mode. After imaging, FRET acceptor photobleaching on selected regions of interest was used as a positive control of FRET efficiency (Fig. S1*B*). Data were analyzed using NIS Elements software (Nikon, Inc.).

Western Blots. Western blots were performed as previously described (26, 28). Whole-cell homogenates were obtained from 10 dissected neural tubes from 26-hpf wild-type embryos, incubated with 100 nM SAG or vehicle only for 4 h, and processed for Western blot assay using anti-Gli3, 1:500 (Abcam). Similarly, neural tubes from mGli2-GFP–expressing embryos were incubated with 100 nM SAG or vehicle only and processed for Western blot assay using anti-Gli2, 1:500 (goat, R&D Systems). For assessing CREB activation, whole-cell homogenates were obtained from 10 dissected spinal cords from 26-hpf wild-type embryos, incubated with 100 nM SAG, 10 μM forskolin, or vehicle only for 30 min and processed for Western blot assay using anti–P-CREB, 1:100 (Cell Signaling). Anti-GAPDH, 1:1,000 (Santa Cruz Biotechnology), and anti-H2B, 1:500 (Cell Signaling), were used as loading controls; secondary antibodies were peroxidase-conjugated (Jackson ImmunoResearch) or fluorophore-conjugated (Life Technologies), 1:5,000.

Immunostaining. Samples were fixed with 4% (wt/vol) paraformaldehyde and processed for immunostaining as previously described (26, 28). Incubations with primary and secondary antibodies were carried out overnight at 4 °C and for 2 h at 23 °C, respectively. Primary antibodies used were anti-Gli2, 1:100 (goat, R&D System); anti-Gli2, 1:200 (rabbit, GeneTex); anti–P-CREB, 1:800 (Cell Signaling); anti-Flag, 1:300 (Sigma); anti-Sox2, 1:300 (R&D Systems); and Alexa Fluor-conjugated secondary antibodies, 1:300 (Life Technologies).

Gli2 Subcellular Localization Dynamics. mGli2-GFP construct was injected into one-cell-stage embryos. Spinal cords from mGli2-GFP–expressing 21-hpf embryos were then dissected, dissociated, and plated in vitro as previously described (26, 28) for 2 h. Cells were imaged every 15 s with a Nikon Swept-field confocal microscope. Regions of interest of the cytosol and nucleus of imaged cells were used to measure changes in mGli2-GFP average fluorescence intensity over time (NIS Elements software, Nikon Instruments Inc.).

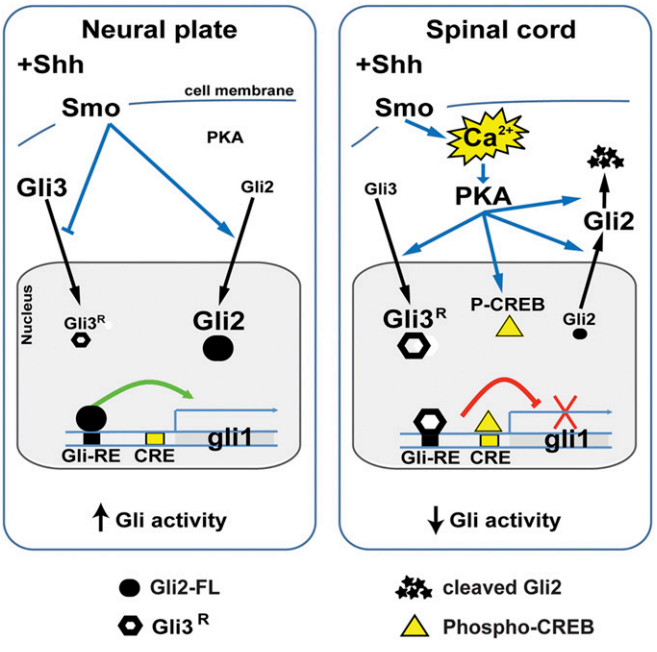

Fig. 5. Model for the mechanism of the switch off in Shh canonical signaling during spinal cord development. The transition from neural plate to spinal cord is accompanied by the appearance of Ca^{2+} spikes, which intercalate in the Shh-signaling pathway to down-regulate Gli activity. This switch off of the canonical Shh pathway is implemented at several levels including regulation of Gli subcellular localization, posttranslational processing, and transcriptional repression, all converging in inhibiting Gli activity.

Drug concentrations used were the following: 100 nM SAG, 10 μM forskolin, 10 nM Shh, 10 μM KT5720 (PKA inhibitor, Tocris), 10 μM dbcAMP (PKA agonist, Tocris), and 100 μM cAMPS-Rp (PKA inhibitor, Tocris).

Antibody Specificity Assays. To prove specificity of anti-Gli2 and anti-Gli3 antibodies used in this study, *X. laevis* Gli2- and Gli3-targeted translation-blocking morpholinos (Gli2-MO: GCACAGAACGCAGGTAATGCTCCAT; Gli3-MO: GACTGGGCTTCCATGTTGTCTTCTC) were unilaterally (Gli2-MO) or bilaterally (Gli3-MO) injected at the two-cell-stage. Embryos were processed for Western blot or immunohistochemistry assays and probed with indicated antibodies.

Data Collection and Statistics. At least five samples were analyzed for each group from at least three independent clutches of embryos. For cell culture experiments, at least 27 cells from at least three independent culture dishes were analyzed per experimental condition. Statistical tests used were paired or unpaired Student's *t* test, $P < 0.05$.

ACKNOWLEDGMENTS. We thank Drs. E. Diaz, N. C. Spitzer, S. Shim, and A. M. Hamilton for comments on previous version of this manuscript; O. A. Balashova for technical advice; and H. Sharma for technical assistance. This work was supported by the Basil O'Connor Starter Scholar Research Award Grant 5-FY09-131 from the March of Dimes Foundation; Klingenstein Foundation Award in Neuroscience; National Science Foundation Grant 1120796; NIH–National Institute of Neurological Disorders and Stroke Grant R01NS073055; Shriners Hospital for Children Grants 86500-Northern California (NCA) and 85220-NCA (to L.N.B.); and a Shriners Postdoctoral Fellowship (to Y.H.B.).

1. Briscoe J, Thérond PP (2013) The mechanisms of Hedgehog signalling and its roles in development and disease. *Nat Rev Mol Cell Biol* 14(7):416–429.
2. Villavicencio EH, Walterhouse DO, Iannaccone PM (2000) The sonic hedgehog-patched-gli pathway in human development and disease. *Am J Hum Genet* 67(5): 1047–1054.
3. Lee J, Platt KA, Censullo P, Ruiz i Altaba A (1997) Gli1 is a target of Sonic hedgehog that induces ventral neural tube development. *Development* 124(13):2537–2552.
4. Balaskas N, et al. (2012) Gene regulatory logic for reading the Sonic Hedgehog signaling gradient in the vertebrate neural tube. *Cell* 148(1-2):273–284.
5. Dessaud E, et al. (2007) Interpretation of the sonic hedgehog morphogen gradient by a temporal adaptation mechanism. *Nature* 450(7170):717–720.
6. Ribes V, Briscoe J (2009) Establishing and interpreting graded Sonic Hedgehog signaling during vertebrate neural tube patterning: The role of negative feedback. *Cold Spring Harb Perspect Biol* 1(2):a002014.
7. Ulloa F, Briscoe J (2007) Morphogens and the control of cell proliferation and patterning in the spinal cord. *Cell Cycle* 6(21):2640–2649.
8. Jacob J, Briscoe J (2003) Gli proteins and the control of spinal-cord patterning. *EMBO Rep* 4(8):761–765.
9. Ruiz i Altaba A, Nguyên V, Palma V (2003) The emergent design of the neural tube: Prepattern, SHH morphogen and GLI code. *Curr Opin Genet Dev* 13(5):513–521.
10. Chamberlain CE, Jeong J, Guo C, Allen BL, McMahon AP (2008) Notochord-derived Shh concentrates in close association with the apically positioned basal body in neural target cells and forms a dynamic gradient during neural patterning. *Development* 135(6):1097–1106.
11. Ingham PW, Taylor AM, Nakano Y (1991) Role of the Drosophila patched gene in positional signalling. *Nature* 353(6340):184–187.
12. Tuson M, He M, Anderson KV (2011) Protein kinase A acts at the basal body of the primary cilium to prevent Gli2 activation and ventralization of the mouse neural tube. *Development* 138(22):4921–4930.
13. Humke EW, Dorn KV, Milenkovic L, Scott MP, Rohatgi R (2010) The output of Hedgehog signaling is controlled by the dynamic association between Suppressor of Fused and the Gli proteins. *Genes Dev* 24(7):670–682.
14. Sheng T, Chi S, Zhang X, Xie J (2006) Regulation of Gli1 localization by the cAMP/protein kinase A signaling axis through a site near the nuclear localization signal. *J Biol Chem* 281(1):9–12.
15. Tukachinsky H, Lopez LV, Salic A (2010) A mechanism for vertebrate Hedgehog signaling: Recruitment to cilia and dissociation of SuFu-Gli protein complexes. *J Cell Biol* 191(2):415–428.
16. Pan Y, Wang C, Wang B (2009) Phosphorylation of Gli2 by protein kinase A is required for Gli2 processing and degradation and the Sonic Hedgehog-regulated mouse development. *Dev Biol* 326(1):177–189.
17. Wang B, Fallon JF, Beachy PA (2000) Hedgehog-regulated processing of Gli3 produces an anterior/posterior repressor gradient in the developing vertebrate limb. *Cell* 100(4):423–434.
18. Spitzer NC, Gu X, Olson E (1994) Action potentials, calcium transients and the control of differentiation of excitable cells. *Curr Opin Neurobiol* 4(1):70–77.
19. Harris GL, Henderson LP, Spitzer NC (1988) Changes in densities and kinetics of delayed rectifier potassium channels during neuronal differentiation. *Neuron* 1(8): 739–750.
20. O'Dowd DK, Ribera AB, Spitzer NC (1988) Development of voltage-dependent calcium, sodium, and potassium currents in Xenopus spinal neurons. *J Neurosci* 8(3): 792–805.
21. Spitzer NC (2006) Electrical activity in early neuronal development. *Nature* 444(7120): 707–712.
22. Borodinsky LN, et al. (2004) Activity-dependent homeostatic specification of transmitter expression in embryonic neurons. *Nature* 429(6991):523–530.
23. De Marco García NV, Karayannis T, Fishell G (2011) Neuronal activity is required for the development of specific cortical interneuron subtypes. *Nature* 472(7343):351–355.
24. Demarque M, Spitzer NC (2010) Activity-dependent expression of Lmx1b regulates specification of serotonergic neurons modulating swimming behavior. *Neuron* 67(2): 321–334.
25. LoTurco JJ, Owens DF, Heath MJ, Davis MB, Kriegstein AR (1995) GABA and glutamate depolarize cortical progenitor cells and inhibit DNA synthesis. *Neuron* 15(6):1287–1298.
26. Swapna I, Borodinsky LN (2012) Interplay between electrical activity and bone morphogenetic protein signaling regulates spinal neuron differentiation. *Proc Natl Acad Sci USA* 109(40):16336–16341.
27. Borodinsky LN, Belgacem YH, Swapna I (2012) Electrical activity as a developmental regulator in the formation of spinal cord circuits. *Curr Opin Neurobiol* 22(4):624–630.
28. Belgacem YH, Borodinsky LN (2011) Sonic hedgehog signaling is decoded by calcium spike activity in the developing spinal cord. *Proc Natl Acad Sci USA* 108(11):4482–4487.
29. Ghosh A, Greenberg ME (1995) Calcium signaling in neurons: Molecular mechanisms and cellular consequences. *Science* 268(5208):239–247.
30. Fan CM, et al. (1995) Long-range sclerotome induction by sonic hedgehog: Direct role of the amino-terminal cleavage product and modulation by the cyclic AMP signaling pathway. *Cell* 81(3):457–465.
31. Hynes M, et al. (1995) Induction of midbrain dopaminergic neurons by Sonic hedgehog. *Neuron* 15(1):35–44.
32. Epstein DJ, Marti E, Scott MP, McMahon AP (1996) Antagonizing cAMP-dependent protein kinase A in the dorsal CNS activates a conserved Sonic hedgehog signaling pathway. *Development* 122(9):2885–2894.
33. Hammerschmidt M, Bitgood MJ, McMahon AP (1996) Protein kinase A is a common negative regulator of Hedgehog signaling in the vertebrate embryo. *Genes Dev* 10(6): 647–658.
34. Mukhopadhyay S, et al. (2013) The ciliary G-protein-coupled receptor Gpr161 negatively regulates the Sonic hedgehog pathway via cAMP signaling. *Cell* 152(1-2): 210–223.
35. Kim J, Kato M, Beachy PA (2009) Gli2 trafficking links Hedgehog-dependent activation of Smoothened in the primary cilium to transcriptional activation in the nucleus. *Proc Natl Acad Sci USA* 106(51):21666–21671.
36. Montminy MR, Bilezikjian LM (1987) Binding of a nuclear protein to the cyclic-AMP response element of the somatostatin gene. *Nature* 328(6126):175–178.
37. Benbrook DM, Jones NC (1994) Different binding specificities and transactivation of variant CRE's by CREB complexes. *Nucleic Acids Res* 22(8):1463–1469.
38. Kornhauser JM, et al. (2002) CREB transcriptional activity in neurons is regulated by multiple, calcium-specific phosphorylation events. *Neuron* 34(2):221–233.
39. West AE, et al. (2001) Calcium regulation of neuronal gene expression. *Proc Natl Acad Sci USA* 98(20):11024–11031.
40. Merz K, Herold S, Lie DC (2011) CREB in adult neurogenesis: Master and partner in the development of adult-born neurons? *Eur J Neurosci* 33(6):1078–1086.
41. Lamph WW, Dwarki VJ, Ofir R, Montminy M, Verma IM (1990) Negative and positive regulation by transcription factor cAMP response element-binding protein is modulated by phosphorylation. *Proc Natl Acad Sci USA* 87(11):4320–4324.
42. Rutberg SE, et al. (1999) CRE DNA binding proteins bind to the AP-1 target sequence and suppress AP-1 transcriptional activity in mouse keratinocytes. *Oncogene* 18(8): 1569–1579.
43. Masquilier D, Sassone-Corsi P (1992) Transcriptional cross-talk: Nuclear factors CREM and CREB bind to AP-1 sites and inhibit activation by Jun. *J Biol Chem* 267(31): 22460–22466.
44. Zhang SJ, et al. (2011) A signaling cascade of nuclear calcium-CREB-ATF3 activated by synaptic NMDA receptors defines a gene repression module that protects against extrasynaptic NMDA receptor-induced neuronal cell death and ischemic brain damage. *J Neurosci* 31(13):4978–4990.
45. Riobo NA, Saucy B, Dilizio C, Manning DR (2006) Activation of heterotrimeric G proteins by Smoothened. *Proc Natl Acad Sci USA* 103(33):12607–12612.
46. Barzi M, Berenguer J, Menendez A, Alvarez-Rodriguez R, Pons S (2010) Sonic-hedgehog-mediated proliferation requires the localization of PKA to the cilium base. *J Cell Sci* 123(Pt 1):62–69.
47. Ruat M, Hoch L, Faure H, Rognan D (2014) Targeting of Smoothened for therapeutic gain. *Trends Pharmacol Sci* 35(5):237–246.
48. Robbins DJ, Fei DL, Riobo NA (2012) The Hedgehog signal transduction network. *Sci Signal* 5(246):re6.
49. Teperino R, et al. (2012) Hedgehog partial agonism drives Warburg-like metabolism in muscle and brown fat. *Cell* 151(2):414–426.
50. Yam PT, Langlois SD, Morin S, Charron F (2009) Sonic hedgehog guides axons through a noncanonical, Src-family-kinase-dependent signaling pathway. *Neuron* 62(3):349–362.
51. Pascual O, et al. (2005) Sonic hedgehog signalling in neurons of adult ventrolateral nucleus tractus solitarius. *Eur J Neurosci* 22(2):389–396.
52. Orellana SA, McKnight GS (1992) Mutations in the catalytic subunit of cAMP-dependent protein kinase result in unregulated biological activity. *Proc Natl Acad Sci USA* 89(10):4726–4730.